JPET #100032

Title Page

Proteomic analysis of rat liver phosphoproteins following treatment with protein kinase

inhibitor H89 (N-(2-[p-bromocinnamylamino-]ethyl)-5-isoquinoline-sulfonamide).

Myrtle A. Davis *, Douglas Hinerfeld , Sajan Joseph , Yu-Hua Hui , Naijia H. Huang ,

John Leszyk, Jennifer Rutherford-Bethard and Sun W.Tam

AFFILIATIONS

Toxicology and Drug Disposition, Lilly Research Laboratories, Eli Lilly and Company,

Greenfield, IN 46140 (MD, SJ, YH & NH)

University of Massachusetts Medical School, Proteomic Consortium, 222 Maple

Avenue, Fuller Building, Shrewsbury, MA 01545 (DH, JL & ST)

Medical University of South Carolina, Department of Pharmacology, 173 Ashley Ave,

BSB, Charleston, SC 29425 (JRB)

1

JPET #100032

Running Title Page

Proteomics of rat liver treated with H89

Document Statistics

Number of text pages- 17

Number of tables = 2

Figures = 4

References = 24

Number of words in Abstract = 228

Number of words in Introduction = 384

Number of words in Discussion = 734

List of abbreviations

MS, mass spectrometry; 2D gel, 2 dimensional gel electrophoresis; MALDI-TOF MS,

matrix assisted laser desorption/ionization-time-of-flight-mass spectrometry; PKA,

protein kinase A.

Section Assignment = Chemotherapy, antibiotics and Gene therapy

2

ABSTRACT

Phosphorylation of kinase targets are the essential measure of kinase inhibitor activity. Therapeutic strategies focused on kinase inhibition rely heavily on surrogate measures of kinase inhibition obtained from in vitro assay systems. There is a need to develop methodology that will facilitate measurement of kinase inhibitor activity or specificity in tissue samples from whole animals treated with these compounds. Many of the current methods are limited by the use of antibodies; many of which do not cross react between several species. The proteomics approach described herein has the potential to reveal novel tissue substrates, potential new pathway interconnections and inhibitor specificity by monitoring differences in protein phosphorylation. We used the protein kinase inhibitor H89 as a tool to ask whether differential profiling of tissue phosphoproteins can be used to detect treatment related effects of a PKA inhibitor *in vivo*. With a combination of phosphoprotein column enrichment, high-throughput 2D gel electrophoresis, differential gel staining with ProQ Diamond/Sypro Ruby, statistical analysis and MALDI-TOF MS analysis, we were able to show clear differences between the phosphoprotein profiles of rat liver protein extract from control and treated animals. Moreover, several proteins that show a potential change in phosphorylation were previously identified as PKA substrates or have putative PKA phosphorylation sites. The data presented support the use of differential proteomic methods to measure effects of kinase inhibitor treatment on protein phosphorylation *in vivo*.

INTRODUCTION

Determining the effects of kinase inhibitors on protein substrates *in vivo* is of

central importance relative to inferences about inhibitor specificity and mechanisms of

observed biological effects. In addition, *in vivo* studies are best suited to represent

metabolism and other physiological parameters likely to influence kinase inhibitor

activity at the organ level. Methods capable of producing data that support target

inhibition *in vivo*, or organ specific protein phosphorylation events are especially

important for whole animal studies. Ultimately, these methods can enable the use of

whole animal studies to translate kinase inhibitor specificity and activity measurements

obtained from biochemical and cell-based screening assays.

H89 (N-(2-[p-bromocinnamylamino-]ethyl)-5-isoquinoline-sulfonamide) is a commercially

available isoquinolinesulfonyl kinase inhibitor (Hidaka et al., 1984). It is purportedly a

potent inhibitor of Protein Kinase A (PKA) although it may have additional kinase

inhibitory activities (Davies et al., 2000; Choi et al., 2001; Makaula et al., 2005). H89

has been widely used as a tool to inhibit PKA in cell-based or biochemical assays,

however mammalian studies using H89 *in vivo* are limited. Short term studies that used

intrathecal, topical, subcutaneous or intracerebroventricular administration have been

reported with durations of treatment ranging from 5 to 120 min (Hua et al., 1999; Dolan

and Nolan, 2001; Vargas et al., 2001; Fang et al., 2003; Li and Chen, 2003; Sun et al.,

2004; Lim et al., 2005). Recently, H89 administration to isolated rat hearts has been

reported (Makaula et al., 2005). We used H89 as a tool to ask whether differential

profiling of tissue phospho-proteins can be used to detect effects of PKA inhibitor

treatment *in vivo*. The data presented support the application of differential proteomic

methods to measure effects of kinase inhibitor treatment on protein phosphorylation *in vivo*. We used standard 2D gel- MALDI-TOF MS analysis technologies in combination with two recently commercialized reagents; Qiagen phospho-protein enrichment column and the phospho-protein specific dye, Pro-Q Diamond stain to analyze proteins from H89 treated rat liver tissues (Schulenberg et al., 2004; Makrantoni et al., 2005; Wu et al., 2005). Using this method, we successfully identified a decrease in phosphorylation of kinase substrates in liver protein extracts from animals treated with the kinase inhibitor, H89. The results presented support the possibility that kinase inhibitor activity can be examined from whole animal studies via differential profiling of phosphoproteins isolated from tissues.

METHODS

A. Chemical compound

N-(2-[P-Bromocinnamylamino]-ethyl)-5-isoquinolinesulfonamide. 2HCl (H89) was purchased from Alexis/AXXORA, San Diego, CA. The compound was made into a 400 mg/ml stock solution in 100% DMSO. Fifty microliters of the 400 mg/ml stock was diluted with 950 microliters of 0.9% sterile saline (1:20 dilution) to make 1.0 ml of dosing solution. The final dosing solution was 5% DMSO and 20 mg/ml 519193 2HCl (H89) for subcutaneous administration. Preparations were made daily for BID dosing.

B. Experimental animals, treatment groups and pharmacokinetic study

All protocols and animal care were approved and performed according to the Institutional Animal Care and Use Committee of Eli Lilly Research Laboratories. Adult male Sprague-Dawley Rats (250 ± 40 g body wt; Harlan Breeding Laboratories) were housed in a temperature-controlled room with a 12:12-h light-dark cycle and fed a standard chow diet throughout their stay in the Animal Facility.

Animals were randomly assigned to one of three treatment groups comprised of six animals per group: Five percent DMSO in 0.9 % sterile saline (vehicle) only, 20 mg/kg H89 in vehicle or 200 mg/kg H89 in vehicle. Animals were dosed twice daily on Test Days 0-2 at approximately 8:00 AM and 1:00 PM. A single dose was administered at approximately 8:30 AM on Test day 3 to accommodate the 12:30 PM necropsy on the day 3. Animals were euthanized by CO_2 chamber and sections from the left lateral lobe of the liver from each animal were clamp frozen with metal clamps pre-chilled in liquid nitrogen. Tissue samples were stored at –80°C until processed for protein analysis.

6

A separate group of animals was used for pharmacokinetic measurements.

Approximately 1.0 ml of whole blood was collected into heparinized collection tubes at

0.5, 1, 4, and 24 hours. after a single dose of 20 or 200 mg/kg H89. Whole blood was

processed to plasma, and plasma samples were stored at below -60°C immediately

after processing until analyzed. Plasma levels of H89 were determined by a standard

protein precipitation and LC/MS/MS detection. Stock solutions (1 mg/ml) of H89 were

prepared in ethanol and were serially diluted with pooled rat plasma to prepare

duplicate standards ranging from 1 to 4000 ng/ml. One set of standards was analyzed

at the beginning and one set at the end of each sample batch. Plasma samples (0.05

ml) in 96-well plates were treated by protein precipitation with the addition of methanol

solution containing an analog internal standard (0.1 mL). The resulting mixtures were

centrifuged at 4000 rpm and 4°C for 10 minutes, and supernatants (0.05 mL) were

transferred to a second 96 well plate for MS injection. The samples were analyzed with

a Sciex API 4000 Triple Quadrupole Mass Spectrometer (Sciex Division of MDS Inc.,

Toronto, Canada) coupled to a Shimadzu HPLC System (LC-IOAD Shimadzu) and a

HTS PAL Leap Autosampler (Leap Technology, Carrboro, NC). Samples (0.01 mL)

were injected onto a HPLC column (5 μm Merck Chromolith SpeedRod, 4.6 x 50 mm)

and eluted with the gradient mode at 45°C. The chromatographic conditions consisted

of a mobile phase A (1000:1 water/88% formic acid, v/v), and mobile phase B (1000:1

MeOH/88% formic acid, v/v) that was run over a 1-min gradient at a flow rate of 1.5

ml/min. A positive ion mode with turbo spray, an ion source temperature of 550°C and a

dwell time of 100 msec was utilized for mass spectrometric detection. Quantitation was

performed using multiple reaction monitoring (MRM) at the 445.92 to 194.83 transitions.

The calibration curves were obtained by plotting the peak area ratio of parent drug to

the internal standard versus drug concentration using linear regression with $1/x^2$

7

weighting. Pharmacokinetic parameters were calculated using a non-compartmental

model.

C. Enrichment for phosphorylated rat liver protein

Phospho-proteins from rat liver were enriched on a Qiagen PhosphoProtein

Purification column by the manufacturer's protocol. Briefly, rat liver protein was

extracted by homogenization in lysis buffer containing 0.25% (w/v) CHAPS,

protease/phosphatase inhibitors and benzonase as described in the manufacture's

protocol (Phosphoprotein Purification Kit, Qiagen Inc. Valencia, CA) for 30 minutes at

4°C and centrifuged at 10,000 x g at 4°C for 30 minutes to remove insoluble material.

Total extracted rat liver protein was diluted to a concentration of 0.1 mg/ml in a total

of 25 ml lysis buffer (described above) and was applied to a lysis buffer-equilibrated

PhosphoProtein purification column at room temperature. After washing the column

with 6.0 ml of lysis buffer, the phospho-proteins were eluted with 2 ml of

PhosphoProtein Elution Buffer. The yield of phosphorylated protein was determined by

the Bradford assay. The flow through samples were passed through 2 additional

columns to insure complete removal of phosphoproteins from the sample. The

phospho-proteins were then concentrated by ultra-filtration in a 10kD cut-off Amicon

Ultra column (Millipore, Billerica, MA).

D. Qiagen PhosphoProtein Purification Column and Pro-Q stain Validation

The Qiagen phosphoprotein column recovery was validated using a standard

phospho-peptide, Pp60 c-src (521-533), # 86-3-11 (American Peptide Company,

Sunnyvale, CA). A seven point standard curve was prepared ranging from 12.5 to 1000

ng and analyzed by LC/UV with the LC Packings capillary LC System with a 100 um

C18 column. 250 ng of the standard peptide was spiked into a 250 mg liver lysate and loaded onto the Qiagen column. The flow through, wash, and eluent were collected and analyzed by LC/UV to determine the amount of peptide retained and recovered from the phosphor-protein enrichment procedure. Standard curves were obtained before and after the flow through, wash, and eluent fractions were injected.

To validate the Pro-Q Diamond stain specificity, four micrograms of the liver protein was solublized in NuPAGE LDS buffer (Invitrogen, Carlsbad CA), reduced with 50 mM Dithiothreitol (DTT) and electrophoresed on a 4-12% Bis-Tris SDS NuPage gel for one hour at 200 volts. The gel was fixed and stained in Pro-Q Diamond by manufacturer's protocol (Molecular Probes, Eugene, OR) and imaged on an Amersham (GE Healthcare, Fairfield, CT) Typhoon laser scanner and then counterstained in Coomassie blue and imaged on a flat bed scanner.

E. Two-dimensional electrophoresis

Prior to isoelectric focusing (IEF), samples were acetone precipitated and solubilized in 40mM Tris, 7M Urea, 2M Thiourea and 2% CHAPS, reduced with tri-butylphosphine, and alkylated with 10mM acrylamide for 90 min at room temperature. Following a second round of acetone precipitation, the pellet was solubilized in 7M Urea, 2M Thiourea and 2% CHAPS (resuspension buffer) and buffered exchange through 10 kD cutoff off Amicon Ultra device with at least two volumes of the resuspension buffer to reduce the conductivity of the sample. Seventy-five micrograms protein were subjected to IEF on 11cm pH 3-10 and pH 4-7 immobilized pH gradient (IPG) strips (Proteome Systems, Sydney, NSW, Australia). All gels were run in triplicate. Following IEF, IPG strips were equilibrated in 6M urea, 2% SDS, 50mM Tris-acetate buffer (pH 7.0), 0.01% bromophenol blue and subjected to SDS polyacrylamide

gel electrophoresis on 6-15% Gel Chips™ (Proteome Systems). All gels were fixed and

stained in Pro-Q Diamond, 60 ml per gel, imaged on the Typhoon scanner and then

stained in Sypro® Ruby ,70 ml per gel, (Molecular Probes, Eugene, OR) and imaged

again on the Typhoon scanner.

F. Image Analysis

Analysis of all gel images was performed using Progenesis Discovery and Pro

(Nonlinear Dynamics Inc. Newcastle upon Tyne, UK). Following spot detection,

matching, background subtraction, normalization and filtering, data for both Pro-Q

Diamond and Sypro Ruby gel images was exported to the Pro Informatics package.

Normalized volumes for all spots were subjected to principle component analysis (PCA).

Pairwise comparisons between groups was performed using the Student's T-test in

Progenesis Discovery to identify spots whose expression was significantly altered ($p <$

.05) due to treatment.

G. Protein digestion and MALDI analysis

Protein spots were automatically detected and excised using the Xcise apparatus

(Shimadzu Biotech, Japan). Gel pieces were washed twice with 150μL 25mM

ammonium bicarbonate, pH 8.2, 50% v/v acetonitrile (ACN) and then dehydrated by the

addition of 100% ACN and then air dried. 30 ng of trypsin (Promega, Madison, WI) in

25 mM ammonium bicarbonate (20 μg/μL) was added to each gel piece and incubated

at 30°C for 16 hours. The peptides were extracted by sonication. The peptide solution

was automatically desalted and concentrated using ZipTips from Millipore (Bedford, MA)

on the Xcise apparatus and spotted onto the Axima (Kratos, Manchester, UK) MALDI

target plate. Peptide mass fingerprints of and Post-source Decay (PSD) tryptic peptides

JPET #100032

were generated by matrix assisted laser desorption/ionization-time-of-flight-mass

spectrometry (MALDI-TOF-MS) using an AximaCFR (Kratos).

H. MS database search

All spectra were automatically analyzed by the BioinformatIQ integrated suite of

bioinformatics tools from Proteome Systems, using a combination of Ioniq and Mascot

searching algorithms. Protein identifications were assigned by comparing peak lists to a

database containing theoretical tryptic digests of NCBI and Swiss Prot sequence

databases. Protein identification was evaluated based on percent coverage, MOWSE

score, number of peptide matches, peak intensity, and match of pI and molecular weight

with the location of the protein on the 2D gel. Post-source Decay (PSD) experiments

were also acquired to confirm protein identifications.

RESULTS:

The pharmacokinetic data from the plasma of the animals are shown in Table 1. As shown, substantial exposure was obtained following 20 and 200 mg/kg SQ Dosing with H89. Following treatment, rat livers were processed according to the schematic in Figure 1. Before applying the liver samples through the Qiagen phosphoprotein column purification, the affinity chromatography column was tested with a phospho-peptide standard to validate specific binding of phosphorylated protein to the column. The flow through, wash, and eluent fractions were analyzed by LC/UV and the amount of peptide retained and recovered from the phosphorylation enrichment procedure was determined. An average recovery of 97.24% of the phospho-peptide with the column was achieved (Figure 2).

Pro-Q Diamond from Molecular Probes Inc is a sensitive new noncovalent fluorescent dye staining technology for the detection of phosphoserine-, phosphothreonine- and phosphotyrosine-containing proteins displayed on SDS-polyacrylamide gels and 2-D gels. Gels were fixed, washed with water, and then stained by incubation in a single solution. The stain can quantify protein loads ranging from 1.0 ng to 1.0 µg on a single electrophoresis gel. The stain was fully compatible with matrix-assisted laser desorption time-of-flight mass spectrometry, thus facilitating protein identification after gel electrophoresis.

Subsequent to Pro-Q Diamond staining, SYPRO Ruby was used to restain the same gel to reveal total protein level. This protein gel stain is a noncovalent stain that does not require aldehyde fixation. As little as 75 fmol of stained protein can be recovered from the gel and accurately identified using MALDI-TOF mass spectrometry. It has a broad

linear quantitation range, extending over three orders of magnitude. These features

made it possible to obtain accurate protein quantitation for both highly expressed and

minimally expressed proteins in the gel. The specificity of the Pro-Q Diamond stain was

also confirmed by analyzing the liver flow-through and eluent from the Qiagen column

by SDS-PAGE. Flow-through and eluent from the Qiagen column was separated by

SDS-PAGE and gels were stained with Pro-Q Diamond. The eluent, consisting of a

concentrated fraction of phosphorylated protein, stained heavily with Pro-Q Diamond

compared to the light staining of the flow through samples, which contained mostly non-

phosphorylated protein (not shown).

After Qiagen column enrichment, each sample was resolved on 2D gel in two pH

ranges, 3-10 and 4-7, in triplicate, and stained with Pro-Q diamond and Sypro Ruby

dyes. Protein separation and gel staining was highly reproducible (Figure 3A and 3B).

Proteins were much better resolved on the narrow-range pH 4-7 gels which is important

to note because changes in phosphorylation status may result in a relatively small

change in a protein's pI. The combined use of ProQ Diamond and the total protein dye,

Sypro Ruby enabled the detection and quantitation of low abundance, but highly

phosphorylated proteins.

To determine whether the 2D gel patterns were able to cluster the samples

according to treatment, the normalized volumes for all spots on the gels were subjected

to PCA analysis. The results of the PCA analysis of the pH 4-7 Sypro Ruby stained

gels revealed distinct classes of samples that clearly reflect the grouping and treatment

of the animals. By compiling the 2D gel overall pattern and applying statistical analysis

to protein spot intensity, we were able to cluster gel images based on the treatment

effect. To identify spots that were differentially phosphorylated in protein extracts from

treated versus the control, Student's t-tests were performed. Eight proteins were

determined to be statistically different ($p < 0.05$) between the control and high dose

groups as shown in Figure 4A. Figure 4B shows the histograms of each protein with

their respective standard deviation of their normalized volume from the triplicate gels.

Phosphorylation of several proteins were increased in kinase inhibitor treated protein

extracts relative to control; while the relative phosphorylation of others decreased.

Detailed quantitative normalized volume of each protein is displayed (Figure 4B).

Eight spots whose expression was significantly changed were subjected to

MALDI-TOF MS analysis to obtain the protein identity. The proteins identified are listed

in Table 2. Four of the protein spots were fructose-1,6-bisphosphatase, indicative of

varying degrees of post-translational modification of the same protein induced by H89

via phosphorylation. On the 2D gels, this protein showed a wide range of pI that

suggests phosphorylation at multiple sites of the same protein. Hybrid MALDI ion

trap/time-of-flight mass spectrometry confirmed the identity and phosphorylation of

Fructose 1-6 bisphosphatase (not shown).

14

DISCUSSION

We identified distinct modifications of protein phosphorylation in protein extracts derived from livers of rats treated with H89. Fructose-1, 6-bisphosphatase is of primary interest and is one of the rate limiting enzymes of gluconeogenesis in liver and its phosphorylation state was potentially altered in H89 treated animals. Fructose-1, 6-bisphosphatase (FBPase) has been reported as a substrate for cAMP/PKA (Murray et al., 1984; Rakus et al., 2003) and Rakus et al., proposed that phosphorylation of FBPase may regulate its activity. PKA phosphorylation of the liver isoform of fructose-2,6-bisphosphatase (an inhibitor of fructose-1,6-bisphosphatase) at serine 32 has been reported (Kurland et al., 2000). Serines 388, 341 and 356 of FBPase have also been reported to be phosphorylation sites for PKA (Ekman and Dahlqvist-Edberg, 1981; Ekdahl, 1987). These data are consistent with the fact that cyclic AMP plays a major, if not primary, role in the regulation of hepatic gluconeogenesis. The relationship between the observed difference in fructose-2,6-bisphosphatase phosphorylation and hepatic metabolism was not determined in this study, but increased expression of hepatic fructose-2,6-bisphosphate resulted in lowered blood glucose levels in normal mice accompanied by increased plasma lactate, triglycerides, and FFAs (Wu et al., 2001). Fructose-1, 6-bisphosphatase was also found to be very sensitive for assessing cadmium-induced nephrotoxicity (Rajanna et al., 1984). Additional work is underway to determine whether the phosphorylation state of this protein family can serve as specific biomarkers of PKA/cAMP pathway modulation in liver and relationship to hepatic glucose metabolism.

We also observed that heterogeneous nuclear ribonucleoprotein (hnRNP) was differentially phosphorylated in H89 treated liver protein extracts. HnRNP proteins play important roles in mRNA processing. Xie et al., reported nucleo-cytoplasmic transport of HnRNP1 was regulated by cAMP-dependent PKA (Xie et al., 2003). They also showed direct phosphorylation of hnRNP on ser16 via PKA activation and demonstrate that phosphorylation of ser 16 modulates the nucleo-cytoplasmic distribution of hnRNP in PC12 cells. An interesting follow-up to these studies will be the effect of H89 on hepatic mRNA processing.

NSFL1 cofactor p47 (p97 cofactor 47) is an accessory protein for the p97-mediated fusion pathway on of the distinct pathways of membrane fusion involved in golgi reassembly during mitosis (Kondo et al., 1997). It is essential for the p97-mediated re-growth of Golgi cisternae from mitotic Golgi fragments, a process restricted to animal cells. Phosphorylation of p47 on serine 140 by cdc2 appears to be important for Golgi disassembly-assembly during the cell cycle (Uchiyama et al., 2003). Recently, Kano et al. reported that maintenance of the ER network requires a process mediated by p97/p47, and cell cycle-dependent morphological changes of the ER network are regulated through phosphorylation/dephosphorylation of p47 (Kano et al., 2005). It is widely recognized that cAMP and protein kinase A (PKA) are required to maintain G2 arrest and that a drop in PKA activity is required for M phase-promoting factor activation. There have been reports of cdc25 being a substrate of PKA (Duckworth et al., 2002). Identification of the specific residue modified by H89 treatment may provide additional evidence of associating camp/PKA, cdc2 and regulation of p47. Thioredoxin domain containing protein 4 precursor and eukaryotic translation initiation factor 4E were also identified as a differential phosphorylated protein in protein extracts from H89

treated liver. Confirmation of regulation of these two proteins by H89 in liver will require

additional study.

The reported specificity of H89 is an important factor in interpreting these data.

In a standard in vitro cell-free assay conducted at 0.1 mM ATP, H89 (at 10 µM) inhibited

eight protein kinases by 80–100% (Davies et al., 2000). IC50 values were determined

for the protein kinases that were inhibited most strongly, and these studies revealed that

three (MSK1, S6K1 and ROCK-II) were inhibited with potency similar to or greater than

that for PKA (Davies et al., 2000). Of the proteins identified in our in vivo study, none of

them appeared to have predicted MSK1, S6K1 or ROCK-II phosphorylation sites, but

there were other protein spots that remain to be identified. It is remarkable that the

proteins with the most robust changes in phosphorylation in samples from H89 treated

animals all have potential regulatory connection to cAMP/PKA. The results presented

support the idea that key information about kinase inhibitor activity can be derived from

whole animal studies via differential profiling of phosphoproteins isolated from tissues.

Furthermore, this method shows promise for identification of substrate biomarkers that

can be used to establish kinase pathway modulation *in vivo.*

17

ACKNOWLEDGEMENTS

We are grateful of the technical assistance from our former colleagues at Charles River Proteomic Services. John Pirro, Tonya Pekar, Mei Loan Nyguen, David Innamorati and Joesph Bonapace have contributed significantly in many aspects of this study.

References

Choi J, Choi BH, Hahn SJ, Yoon SH, Min DS, Jo Y and Kim M (2001) Inhibition of Kv1.3 channels by H-89 (N--[2-(p-bromocinnamylamino)ethyl]-5-isoquinolinesulfonamide) independent of protein kinase A. *Biochem Pharmacol* **61**:1029-1032.

Davies SP, Reddy H, Caivano M and Cohen P (2000) Specificity and mechanism of action of some commonly used protein kinase inhibitors. *Biochem J* **351**:95-105.

Dolan S and Nolan AM (2001) Biphasic modulation of nociceptive processing by the cyclic AMP-protein kinase A signalling pathway in sheep spinal cord. *Neurosci Lett* **309**:157-160.

Duckworth BC, Weaver JS and Ruderman JV (2002) G2 arrest in Xenopus oocytes depends on phosphorylation of cdc25 by protein kinase A. *Proc Natl Acad Sci U S A* **99**:16794-16799.

Ekdahl KN (1987) Rat liver fructose-1,6-bisphosphatase. Identification of serine 338 as a third major phosphorylation site for cyclic AMP-dependent protein kinase and activity changes associated with multisite phosphorylation in vitro. *J Biol Chem* **262**:16699-16703.

Ekman P and Dahlqvist-Edberg U (1981) The kinetics of unphosphorylated, phosphorylated and proteolytically modified fructose bisphosphatase from fat liver. *Biochim Biophys Acta* **662**:265-270.

Fang L, Wu J, Lin Q and Willis WD (2003) Protein kinases regulate the phosphorylation of the GluR1 subunit of AMPA receptors of spinal cord in rats following noxious stimulation. *Brain Res Mol Brain Res* **118**:160-165.

Hidaka H, Inagaki M, Kawamoto S and Sasaki Y (1984) Isoquinolinesulfonamides, novel and potent inhibitors of cyclic nucleotide dependent protein kinase and protein kinase C. *Biochemistry* **23**:5036-5041.

Hua XY, Chen P and Yaksh TL (1999) Inhibition of spinal protein kinase C reduces nerve injury-induced tactile allodynia in neuropathic rats. *Neurosci Lett* **276**:99-102.

Kano F, Kondo H, Yamamoto A, Tanaka AR, Hosokawa N, Nagata K and Murata M (2005) The maintenance of the endoplasmic reticulum network is regulated by p47, a cofactor of p97, through phosphorylation by cdc2 kinase. *Genes Cells* **10**:333-344.

Kondo H, Rabouille C, Newman R, Levine TP, Pappin D, Freemont P and Warren G (1997) p47 is a cofactor for p97-mediated membrane fusion. *Nature* **388**:75-78.

Kurland IJ, Chapman B and El-Maghrabi MR (2000) N- and C-termini modulate the effects of pH and phosphorylation on hepatic 6-phosphofructo-2-kinase/fructose-2,6-bisphosphatase. *Biochem J* **347**:459-467.

Li KC and Chen J (2003) Differential roles of spinal protein kinases C and a in

development of primary heat and mechanical hypersensitivity induced by

subcutaneous bee venom chemical injury in the rat. *Neurosignals* **12**:292-301.

Lim G, Wang S and Mao J (2005) cAMP and protein kinase A contribute to the

downregulation of spinal glutamate transporters after chronic morphine. *Neurosci

Lett* **376**:9-13.

Makaula S, Lochner A, Genade S, Sack MN, Awan MM and Opie LH (2005) H-89, a

non-specific inhibitor of protein kinase A, promotes post-ischemic cardiac

contractile recovery and reduces infarct size. *J Cardiovasc Pharmacol* **45**:341-

347.

Makrantoni V, Antrobus R, Botting CH and Coote PJ (2005) Rapid enrichment and

analysis of yeast phosphoproteins using affinity chromatography, 2D-PAGE and

peptide mass fingerprinting. *Yeast* **22**:401-414.

Murray KJ, El-Maghrabi MR, Kountz PD, Lukas TJ, Soderling TR and Pilkis SJ (1984)

Amino acid sequence of the phosphorylation site of rat liver 6-phosphofructo-2-

kinase/fructose-2,6-bisphosphatase. *J Biol Chem* **259**:7673-7681.

Rajanna B, Hobson M, Reese J, Sample E and Chapatwala KD (1984) Chronic hepatic

and renal toxicity by cadmium in rats. *Drug Chem Toxicol* **7**:229-241.

Rakus D, Zarzycki M and Dzugaj A (2003) Rabbit muscle fructose-1,6-bisphosphatase is phosphorylatedin vivo. *Acta Biochim Pol* **50**:115-121.

Schulenberg B, Goodman TN, Aggeler R, Capaldi RA and Patton WF (2004) Characterization of dynamic and steady-state protein phosphorylation using a fluorescent phosphoprotein gel stain and mass spectrometry. *Electrophoresis* **25**:2526-2532.

Sun RQ, Tu YJ, Lawand NB, Yan JY, Lin Q and Willis WD (2004) Calcitonin gene-related peptide receptor activation produces PKA- and PKC-dependent mechanical hyperalgesia and central sensitization. *J Neurophysiol* **92**:2859-2866.

Uchiyama K, Jokitalo E, Lindman M, Jackman M, Kano F, Murata M, Zhang X and Kondo H (2003) The localization and phosphorylation of p47 are important for Golgi disassembly-assembly during the cell cycle. *J Cell Biol* **161**:1067-1079.

Vargas ML, Abella C and Hernandez J (2001) Diazepam increases the hypothalamic-pituitary-adrenocortical (HPA) axis activity by a cyclic AMP-dependent mechanism. *Br J Pharmacol* **133**:1355-1361.

Wu C, Okar DA, Newgard CB and Lange AJ (2001) Overexpression of 6-phosphofructo-2-kinase/fructose-2, 6-bisphosphatase in mouse liver lowers blood glucose by suppressing hepatic glucose production. *J Clin Invest* **107**:91-98.

22

Wu J, Lenchik NJ, Pabst MJ, Solomon SS, Shull J and Gerling IC (2005) Functional

characterization of two-dimensional gel-separated proteins using sequential

staining. *Electrophoresis* **26**:225-237.

Xie J, Lee JA, Kress TL, Mowry KL and Black DL (2003) Protein kinase A

phosphorylation modulates transport of the polypyrimidine tract-binding protein.

Proc Natl Acad Sci U S A **100**:8776-8781.

23

Footnotes

Corresponding Author

Myrtle Davis

Toxicology and Drug Disposition, Lilly Research Laboratories,

Eli Lilly and Company,

Greenfield, IN 46140

Ph-317-655-1858

Fax-317 277 6770

E-mail - davisma@lilly.com

JPET #100032

Legends for Figures.

Figure 1: Outline of sample processing scheme.

Figure 2: Validation of Pro-Q Diamond phospho-specific stain. The affinity chromatography column was tested with a phospho-peptide standard to validate specific binding of phosphorylated protein to the column. An average recovery of 97.24% of the phospho-peptide with the column was achieved. Pre = pink line; post = black line.

Figure 3: Selection of PI range and confirmation of Reproducible Protein separation and staining. **A**. Three replicated 2D- gels stained with Pro-Q Diamond and Sypro Ruby using a broad pI range of 3 to 10. **B**: Spot detection and resolution enhancement among 3 replicated 2D-gels stained with Pro-Q Diamond and Sypro Ruby dyes (zoom pI range of 3 to 10). Pro-Q Diamond = pro- ; Sypro Ruby = Ruby. **C:** Comparison of protein phosphorylation and total protein expression in a selected gel region (spot 183). Spot 183 is demonstrable of how combined use of ProQ Diamond and the total protein dye, Sypro Ruby enabled the detection and quantitation of low abundance, but highly phosphorylated protein.

Figure 4: Comparison of protein phosphorylation based on Pro-Q Diamond Staining intensity. **A**. Representative 2D gels (pI 4-7) stained with of Pro-Q diamond. Eight proteins were determined to be statistically different (p<0.05) between the three groups as shown. Phosphorylation of several proteins were increased in kinase inhibitor treated protein extracts relative to control (e.g. 168, 276 313) and others decreased relative to control (e.g. 317,324,474). **B**. Normalized volumes of protein spots

25

calculated from spot intensity per unit area are shown; 1 = vehicle control; 2 = 20 mg/kg

H89; 3 = 200 mg/kg H89 (as detailed in the methods section). **C**. Statistical analysis of

normalized volume among selected proteins spots. Standard deviation of normalized

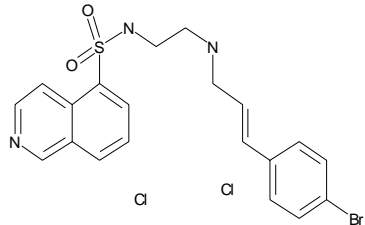volume has been bracketed.

Table 1:

Exposure Data for H89 Following A Single Subcutaneous Dose			Compound Structure
Dose (mg/kg)	20	200	
AUC (ng*hr/mL)	6489.99	71076.25	
AUCtoInf	6951.06	78464.97	
MRT (hr)	6.84	8.23	
Halflife (hr)	6.78	8.12	
Cmax (ng/mL)	436	6525	
Tmax (hr)	4	0.5	

27

Table 2. Proteins identified by MALDI-TOF MS analysis.

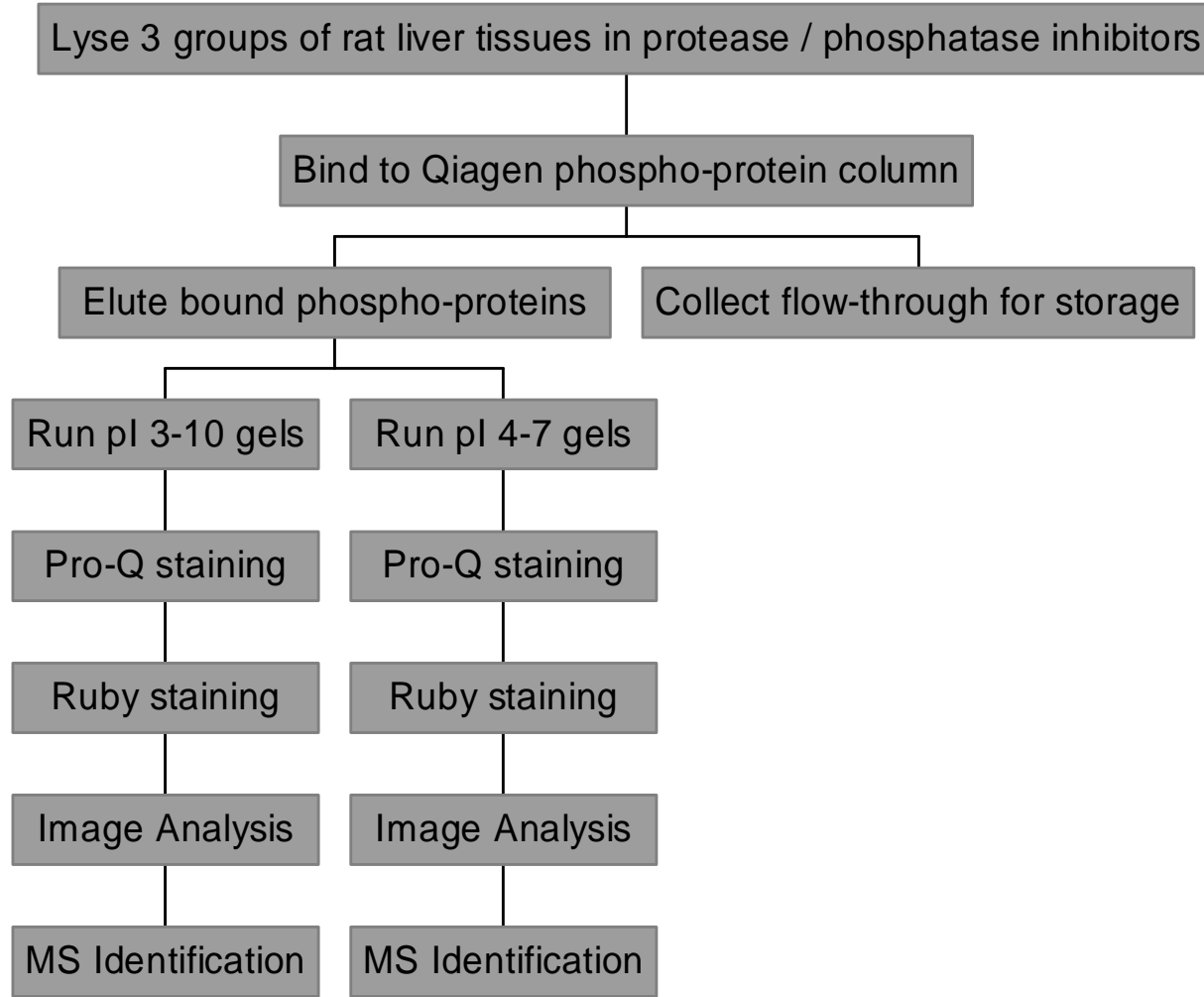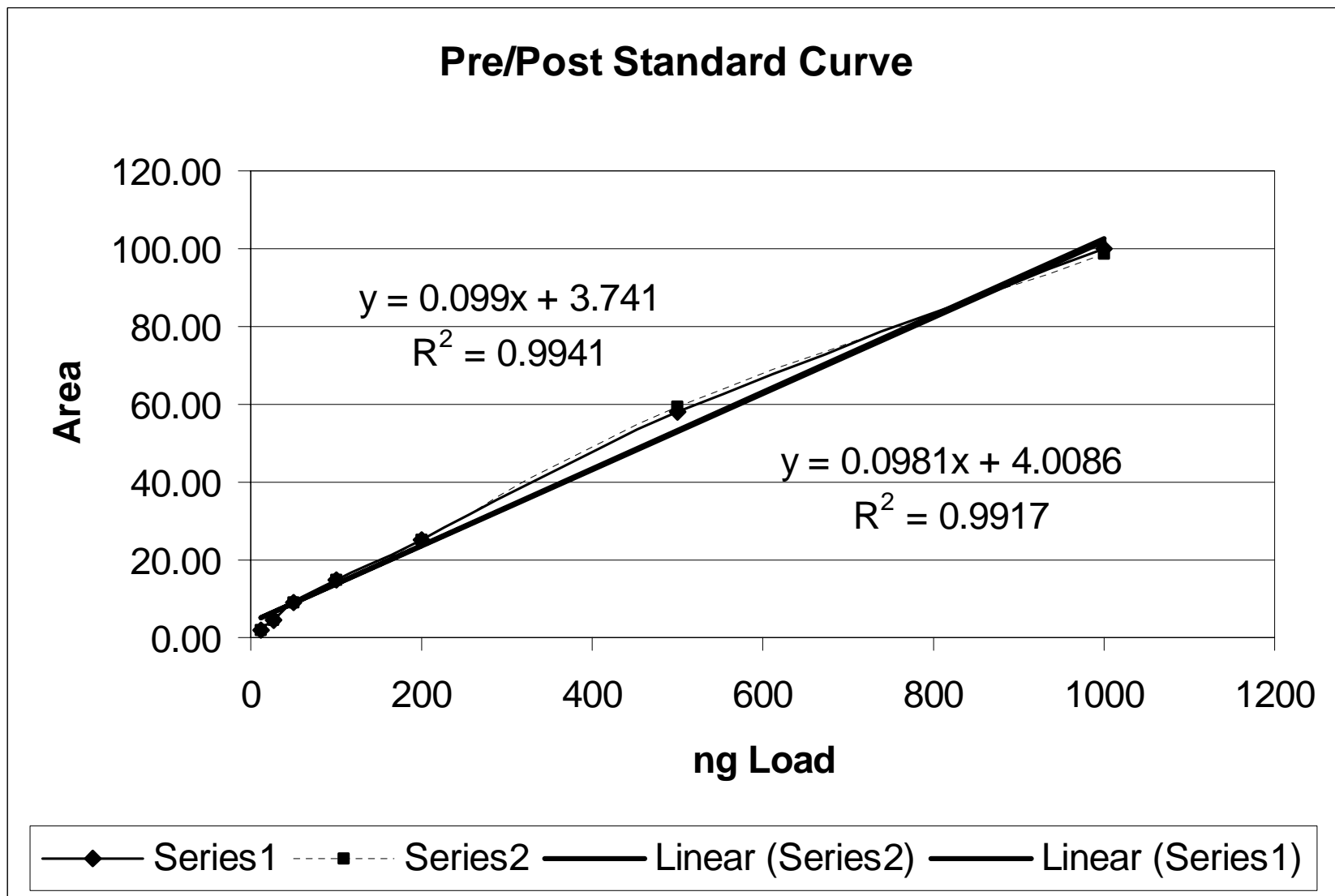| Progenesis Spot #	Protein	Accession #	Species	Mass (kDa)	Search Algorithm
168	Heterogeneous nuclear ribonucleoprotein K (hnRNP K) (DC-stretch binding protein) (CSBP) (Transformation upregulated nuclear	Q07244.30	Homo Sapiens	50.9	Ioniq/Mascott
276	Thioredoxin domain containing protein 4 precursor (Endoplasmic reticulum protein ERp44)	Q9D1Q6.42	Mus musculus	46.8	Ioniq/Mascott
291	NSFL1 cofactor p47 (p97 cofactor p47) (XYbody-associated protein XY40)	O35987.43	Rattus Norvegicus	40.6	Ioniq/Mascott
310	Fructose-1,6-bisphosphatase (EC 3.1.3.11) (D-fructose-1,6-bisphosphate 1-phosphohydrolase) (FBPase)	P19112.16	Rattus Norvegicus	39.4	Ioniq/Mascott
313	Fructose-1,6-bisphosphatase (EC 3.1.3.11) (D-fructose-1,6-bisphosphate 1-phosphohydrolase) (FBPase)	P19112.16	Rattus Norvegicus	39.4	Ioniq/Mascott
317	Fructose-1,6-bisphosphatase (EC 3.1.3.11) (D-fructose-1,6-bisphosphate 1-phosphohydrolase) (FBPase)	P19112.16	Rattus Norvegicus	39.4	Ioniq/Mascott
324	Fructose-1,6-bisphosphatase (EC 3.1.3.11) (D-fructose-1,6-bisphosphate 1-phosphohydrolase) (FBPase)	P19112.16	Rattus Norvegicus	39.4	Ioniq/Mascott
474	Eukaryotic translation initiation factor 4E (eIF-4E) (eIF4E) (mRNA cap-binding protein) (eIF-4F 25 kDa subunit	P20415.33	Mus musculus	25	Ioniq/Mascott

28

Figure 1

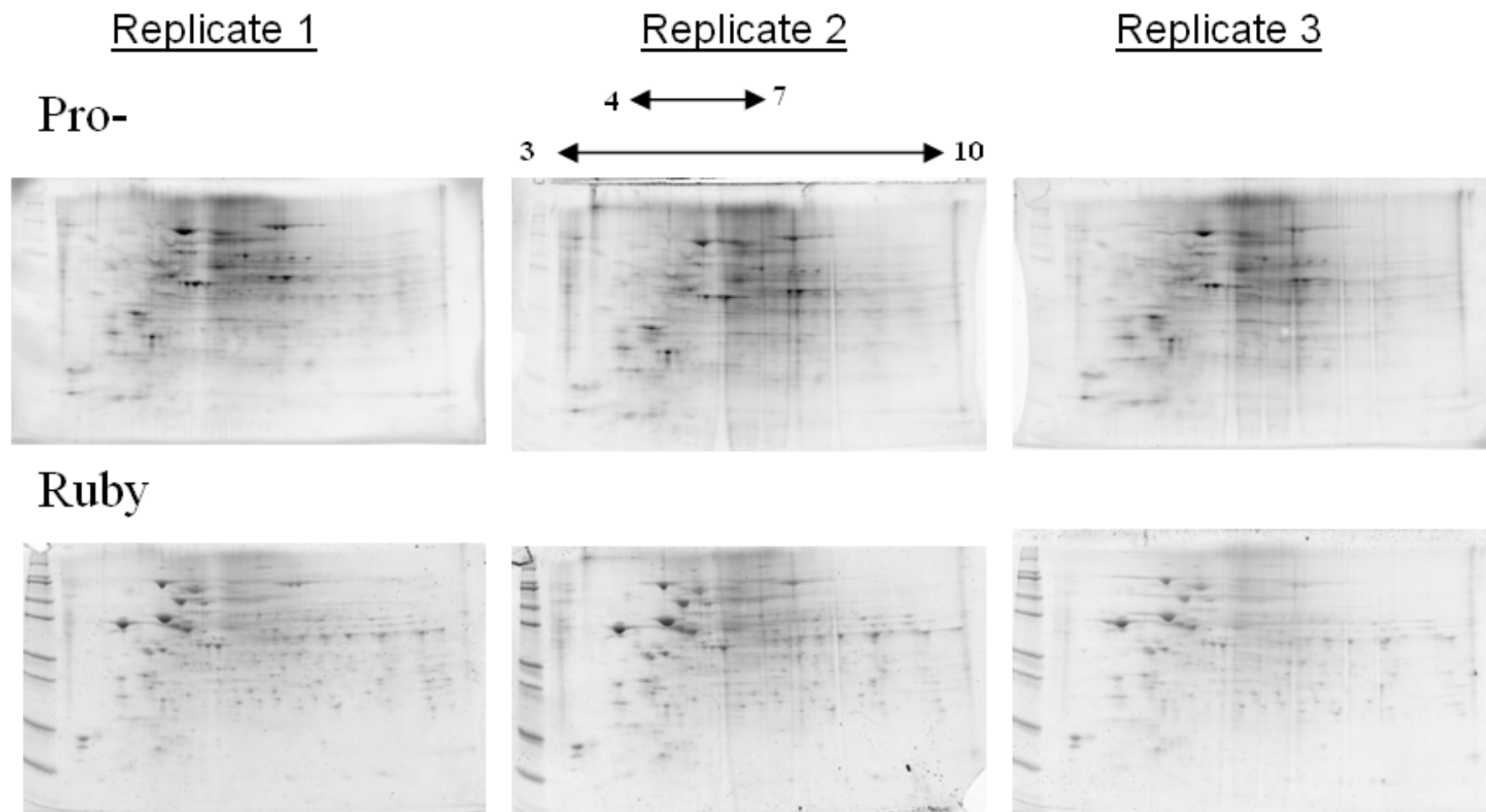**Figure 2.**

Pre/Post Standard Curve

$y = 0.099x + 3.741$

$R^2 = 0.9941$

$y = 0.0981x + 4.0086$

$R^2 = 0.9917$

Area

ng Load

◆ Series1 ■ Series2 ── Linear (Series2) ── Linear (Series1)

Figure 3A

Replicate 1　　　　Replicate 2　　　　Replicate 3

Pro-

4 ⟷ 7

3 ⟷ 10

Ruby

Figure 3B

Pro-

Ruby
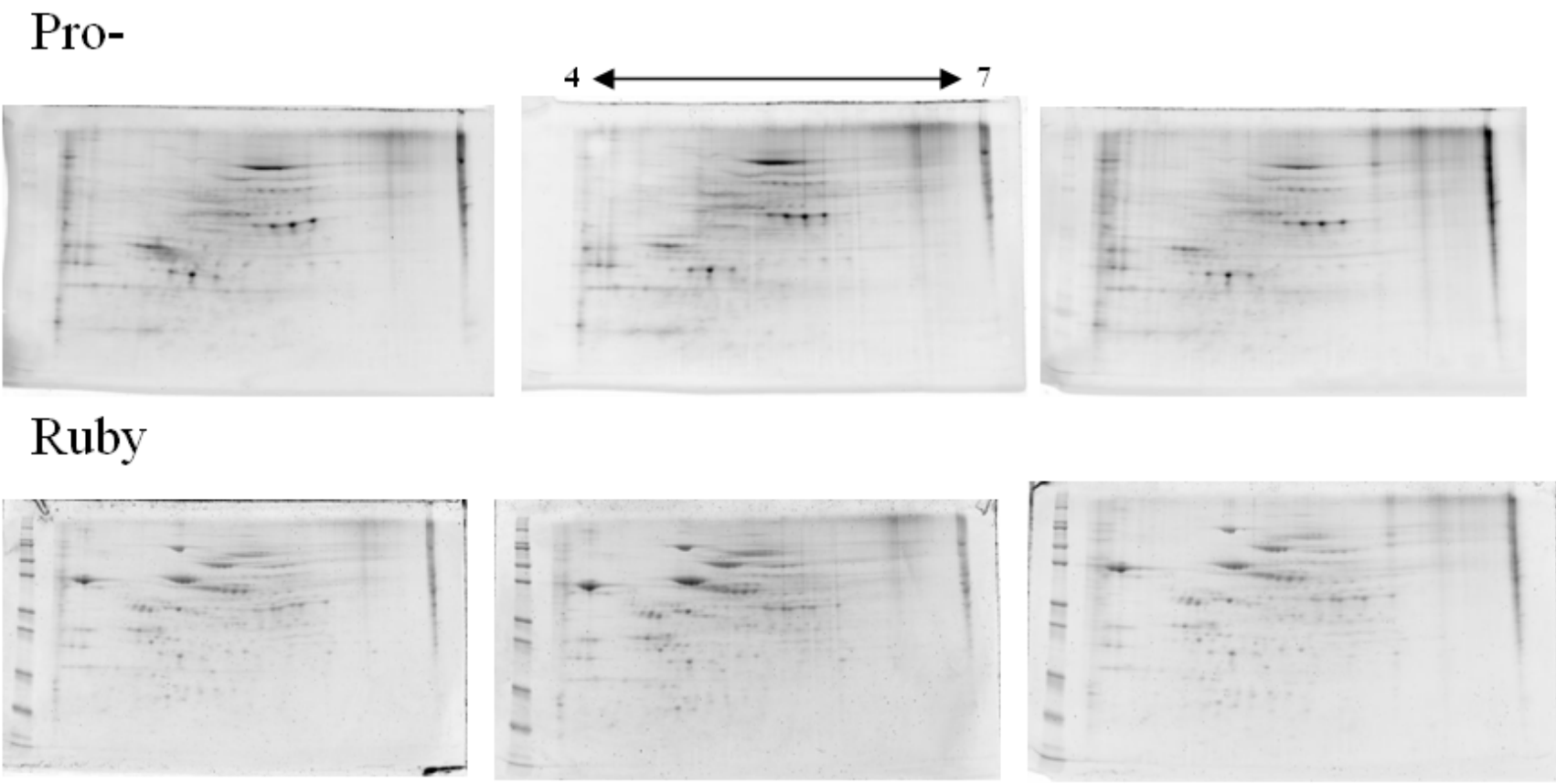
Figure 4A
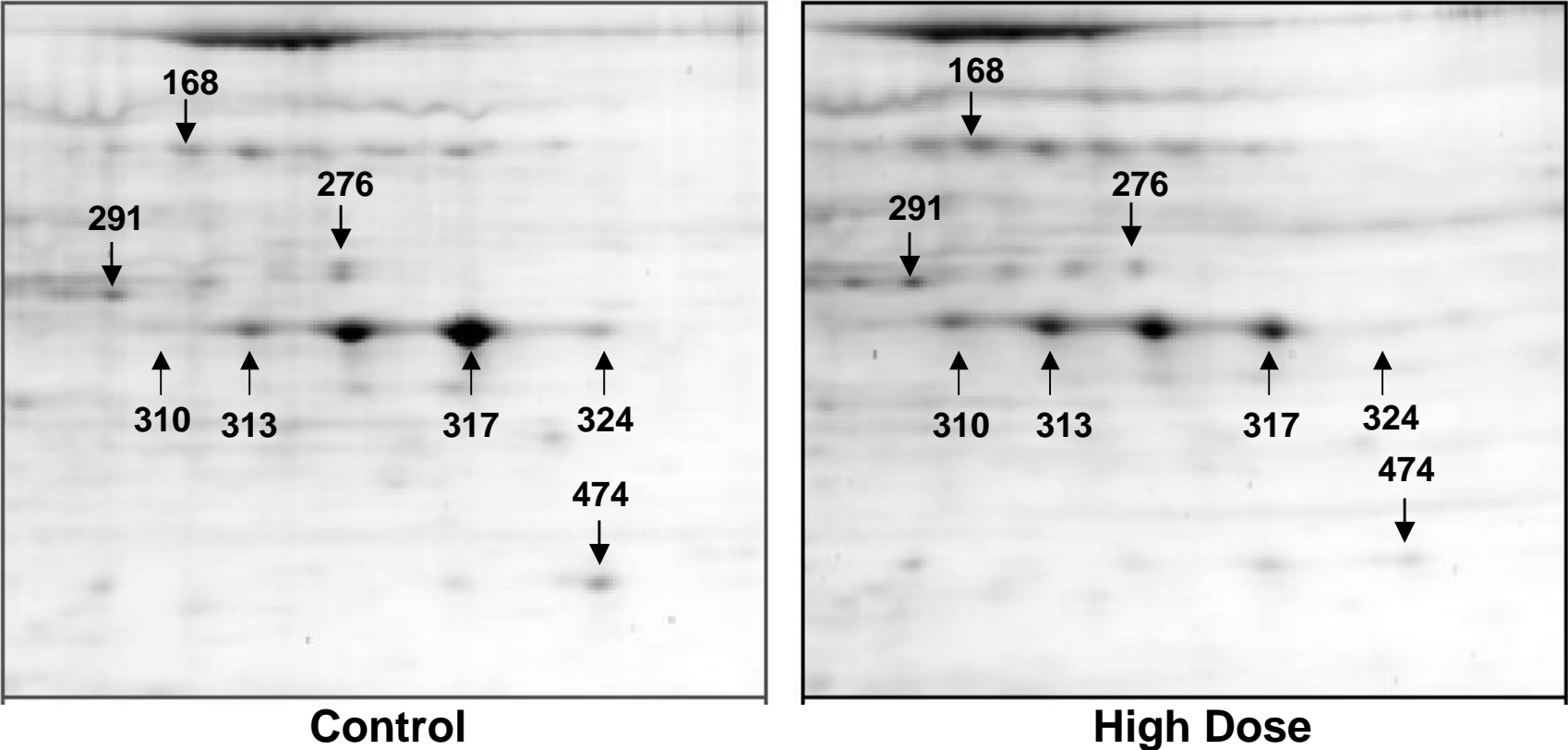
Control

High Dose

Figure 4b
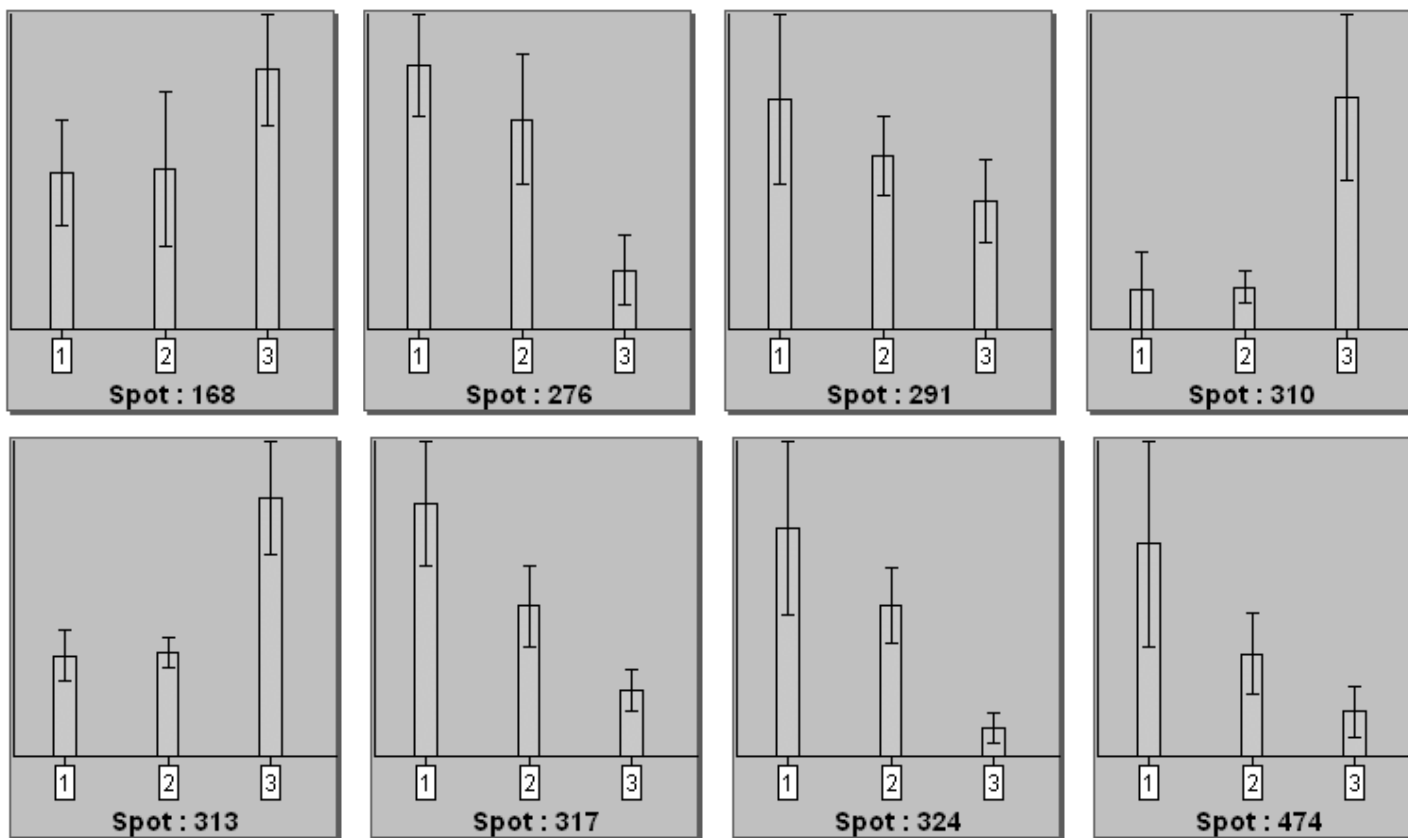
Spot Number	Control	Low Dose	High Dose
317	8.475 (2.099)	5.039 (1.368)	2.234 (0.684)
313	1.216 (0.306)	1.250 (0.185)	3.128 (0.681)
291	0.966 (0.355)	0.725 (0.166)	0.539 (0.172)
324	0.628 (0.238)	0.414 (0.103)	0.077 (0.041)
276	0.537 (0.104)	0.428 (0.133)	0.120 (0.071)
168	0.488 (0.166)	0.498 (0.240)	0.808 (0.173)
474	0.309 (0.149)	0.149 (0.060)	0.065 (0.037)
310	0.195 (0.191)	0.209 (0.081)	1.162 (0.415)